A&A 388, 298–308 (2002)
DOI: 10.1051/0004-6361:20020504

Astronomy & Astrophysics

Hα spectroscopy and BV photometry of RT Lacertae⋆,⋆⋆

A. Frasca[1], Ö. Çakırlı[2], S. Catalano[1], C. İbanoğlu[2], E. Marilli[1], S. Evren[2], and G. Taş[2]

[1] Osservatorio Astrofisico di Catania, via S. Sofia 78, 95123 Catania, Italy
[2] Ege University Observatory, Bornova, İzmir, Turkey
e-mail: afr, scat, ema@ct.astro.it; cakirli,ibanoglu@astronomy.sci.ege.edu.tr

Received 8 January 2002 / Accepted 19 March 2002

Abstract. Contemporaneous spectroscopic and photometric BV observations of the RS CVn type eclipsing binary RT Lacertae were performed in summer 2000. The photometric observations were obtained at the Ege University Observatory, while the spectroscopic ones were carried out at Catania Astrophysical Observatory in the spectral range 5860–6700 Å. We obtained a high quality radial velocity curve of the system that allowed us to give more accurate values of the orbital parameters. A steady decrease of the barycentric velocity from 1920 to 2000 has been pointed out and has been discussed in the context of a third body hypothesis. Through the subtraction of a "synthetic" spectrum, built up with spectra of inactive standard stars, we detected Hα excess emission which fills in the photospheric absorption profiles of both components. With the exception of a few spectra, taken close to the eclipses, in which some extra absorption or a faint double-peaked broad emission appears, there is no further evidence of circumstellar matter in this system, as suggested in previous works. The hotter and more massive star appears also as the more active at a chromospheric level, since it has a Hα flux about ten times greater than the companion, on average. Rotational modulation of the Hα emission has been detected in both stars. The hemisphere of the more massive star facing the observer at phase $0\overset{p}{.}75$ appears brighter (in Hα) than that seen at phase $0\overset{p}{.}25$, while for the less massive G9 IV star the maximum Hα emission is seen around phase $0\overset{p}{.}0$–$0\overset{p}{.}1$. From the analysis of the contemporaneous light curve (Lanza et al. 2002), the more massive G5 IV star results to be more active than the companion at a photospheric level, in agreement with the chromospheric behaviour observed in Hα. In addition, the starspots of the G5 IV star are mainly located in the Hα brighter hemisphere, suggesting a close spatial association of spots and plages in this star. The G9 IV star displays instead the maximum Hα emission at the phase of maximum visibility of the smaller spotted area found from the light-curve analysis. The minimum Hα emission occurs when the more heavily spotted region is visible.

Key words. stars: activity – stars: binaries: spectroscopic – stars: late-type – stars: starspots – stars: individual: RT Lac

1. Introduction

RT Lacertae, included in the list of close binaries with Ca II H and K emission by Popper (1942, 1976), is a double-lined spectroscopic/eclipsing binary classified as an RS CVn system by Hall (1976). It displays a number of peculiarities. In addition to the typical distortion wave, the system appears bluer at the primary minimum and redder at secondary, indicating that the component of lower surface brightness, earlier classified as K1 IV, is bluer than its companion of spectral type G9 IV (Milone 1977). The primary minimum is apparently wider than the secondary and IR excess in the JHKL bands has a phase-dependent component (Milone 1976). These properties have led to the hypothesis of a circumstellar envelope or mass flow in the system (see e.g. Milone 1977; Milone & Naftilan 1980).

Eaton & Hall (1979) proposed a model in which the more massive star is so heavily spotted that its average surface flux, despite its higher temperature, is fainter than that of the cooler star, and it is responsible for the intrinsic variability of the system. Moreover, from long-term broad-band photometric monitoring, Evren (1989) found that both components are active.

Popper (1991), combining photometric and spectroscopic data, classified the two components as approximately G5 for the hotter and G9 IV for the cooler component. According to this picture, the hotter star is also more massive and smaller than the cooler one and displays a very high activity level, with 30–50% of its

Send offprint requests to: A. Frasca, e-mail: afr@ct.astro.it
⋆ Based on observations collected at Catania Astrophysical Observatory, Italy, and at Ege University Observatory, Turkey.
⋆⋆ Table 1 only available at the CDS via anonymous ftp to cdsarc.u-strasbg.fr (130.79.128.5) or via http://cdsweb.u-strasbg.fr/cgi-bin/qcat?J/A+A/388/298

photosphere covered by starspots. The cooler less massive companion is nearly filling its Roche lobe limit and contributes two-thirds of the observed flux at V and red wavelengths (see also Huenemoerder & Barden 1986). Low and intermediate resolution optical spectroscopy, performed by Huenemoerder (1985, 1988) and Huenemoerder & Barden (1986), showed a large range of activity in the Hα line. Their study revealed that the more massive component usually has H_β and H_α excess emission, while the less massive component has excess emission near phase 0.7 at that time. During active times the excess emission exhibited great variations with phase and seemed to come from an extended region. The emission from the more massive component was generally stronger than that of the less massive one. Excess Hα absorption was observed around at phase $0\overset{\text{p}}{.}5$ and remained right through the secondary eclipse, even when the more massive star was occulted. Huenemoerder & Barden (1986) proposed a gas-stream scenario with mass exchange through the inner Lagrangian point, and suggested that this is the primary cause of the Hα activity in RT Lac.

Both components display Ca II H & K emission cores, and the less massive component usually shows weaker emission (Popper 1942, 1991). However, comparable intensities of the Ca II emission lines from both components have been also observed (Armentia et al. 1990).

In this paper, we focus on the spectroscopic Hα behaviour with the orbital phase, with the aim of distinguishing the activity signs of the two components from possible effects of mass transfer and/or circumstellar matter that are frequently observed in semi-detached binary systems of the Algol type. The analysis of a nearly simultaneous light curve will allow us to study the surface inhomogeneities at two atmospheric layers, i.e. photosphere and chromosphere.

Section 2 summarizes the observations and data reductions. In Sect. 3.1, the new radial velocity curve and the analysis of the orbital parameters is presented. In Sects. 3.2 and 3.3 we analyze the Hα emission and its variation together with the main results from contemporaneous photometry. The last section contains conclusions.

2. Observations

2.1. Photometry

RT Lac was observed in B and V Johnson bands on 16 nights from July 12th to November 21st, 2000 at the Ege University Observatory.

The observations were made with the 48-cm Cassegrain telescope to which an SSP5A type photometer, including an unrefrigrated Hamamatsu R4457 PMT, was attached. The stars BD +43° 4108 (HD 209219) and BD +43° 4109 (HD 209220) were taken as comparison and check stars, respectively, to obtain differential magnitudes. The average standard deviation of the observed points is $\pm 0\overset{\text{m}}{.}006$ and $\pm 0\overset{\text{m}}{.}007$ for V and B, respectively.

The new ephemeris for epoch 2000 has been derived from times of minima by İbanoğlu et al. (2001) as:

$$\text{Min I} = \text{JD (Hel) } 24\,51733.2839 + 5\overset{\text{d}}{.}0739900\ E. \quad (1)$$

the smaller and more massive component of RT Lac being in front of the observer at phase zero.

The new photometric solution by Lanza et al. (2002) has pointed out, as already proposed by previous works, that the primary (more massive) star is also the hotter one and the true primary minimum would be at phase $0\overset{\text{p}}{.}5$. Consequently, they give a new ephemeris in which the more massive component is behind the companion at phase $0\overset{\text{p}}{.}0$. In the present paper, however, we will adopt the ephemeris of Eq. (1) in order to maintain consistency with all previous spectroscopic and photometric works.

The individual values of differential magnitude in B and V filters as a function of heliocentric Julian Day are reported in Table 1[1].

2.2. Spectroscopy

The spectroscopic observations were carried out between July 17th and September 24th, 2000 at the *M.G. Fracastoro station* (Mt. Etna, Italy) of Catania Astrophysical Observatory with the REOSC echelle spectrograph fed by the 91-cm telescope through an UV-NIR fiber of 200 μm core diameter. The observations were obtained using the echelle cross-dispersion configuration based on a 900 lines/mm echellette grating and the echelle grating with 79 lines/mm.

The data were acquired with a 1024 × 1024 SITe thinned back-illuminated CCD of 24 × 24 μm pixel size, yielding a spectral range (in 5 orders) from approximately 5860 Å to 6700 Å, and a dispersion of 0.16 Å per pixel. For all the observing runs the width of the slit was set to 550 μm, projected onto 2.7 pixels of the detector, providing a spectral resolving power $\lambda/\Delta\lambda = 14\,000$.

Eighteen spectra of RT Lac were collected during the 16 observing nights. We used μ Her (G5 IV) and ϵ Cyg (K0 III) as standard stars to mimic the hotter and cooler component, respectively. Typical exposure times for the RT Lac spectroscopic observations were between 2400 and 3600 s. The signal-to-noise ratio (S/N) achieved was between 50 and 100, depending on atmospheric condition. 31 Aql (G7 IV) was observed during each run as a radial-velocity standard star.

The data reduction, including bias, scattered light and flat field corrections, extraction of spectral orders and wavelength calibration, was performed on the raw images with the IRAF[2] (Image Reduction and Analysis Facilities) software. For the wavelength calibration the emission lines of a Th-Ar lamp were used.

[1] Available only in electronic form at the CDS.

[2] IRAF is distributed by the National Optical Astronomy Observatory, which is operated by the Association of the Universities for Research in Astronomy, inc. (AURA) under cooperative agreement with the National Science Foundation.

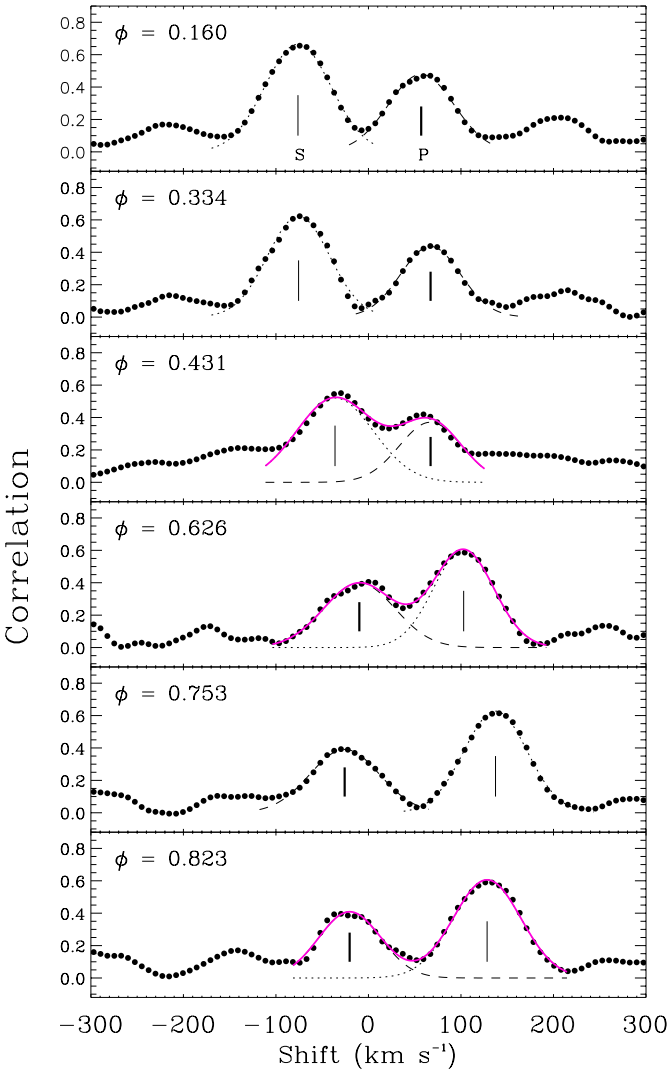

Fig. 1. Sample of Cross Correlation Functions (CCFs) between RT Lac and template spectra (31 Aql) at different phases (dots). The Gaussian fits to the two peaks are displayed with a dotted line for the less massive component (S) and with a dashed line for the more massive one (P). The thick grey line displays the sum of the two Gaussians in more blended cases.

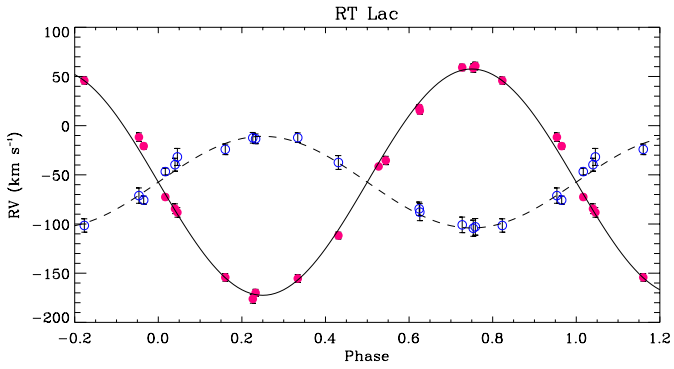

Fig. 2. The radial velocity curve of RT Lacertae. Open circles: RVs of the hotter more massive component. Filled circles: RVs of the cooler less massive one. The best-fit solutions are drawn with dashed and continuous lines for the more massive and less massive component, respectively.

3. Results and discussion

3.1. Radial velocity curve of RT Lac

The radial velocity (RV) measurements of RT Lac were obtained by cross-correlation of each echelle order of RT Lac's spectra with spectra of the bright radial velocity standard star 31 Aql (G7 IV), whose radial velocity is -100.5 km s^{-1} (Evans 1967). For this purpose the IRAF task FXCOR, that computes RVs by means of the cross-correlation technique, was used.

The wavelength ranges for the cross-correlation were selected to exclude the Hα and Na I D_2 lines, which are contaminated by chromospheric emission. The spectral regions heavily affected by telluric lines (e.g. the λ 6276−λ 6315 band of O_2) were also excluded.

Figure 1 shows examples of cross-correlation functions (CCFs) at various orbital phases. The two peaks, more or less blended, correspond to each component of RT Lac. The stronger peak in each CCF corresponds to the less massive, bigger component that has a larger contribution to the observed spectrum at red wavelengths. To better evaluate the centroids of the peaks (i.e. the radial velocity difference between target and template) we adopted two separate Gaussian fits for the cases of significant peak separation (i.e. near the quadratures), and a two-Gaussian fit algorithm to resolve cross-correlation peaks in blended situations.

The radial velocity measurements, listed in Table 2 together with their standard errors, are weighted means of the individual values deduced from each order. The usual weight $W_i = \frac{1}{\sigma_i^2}$ has been given to each measure.

The standard errors of the weighted means have been computed on the basis of the errors σ_i in the RV values for each order according to the usual formula (see e.g. Topping 1972). The latter are computed by FXCOR according to the fitted peak height and the antisymmetric noise as described by Tonry & Davis (1979).

The observational points and their error bars are displayed in Fig. 2 as a function of orbital phase (dots for the cooler less massive star and open circles for the hotter one) as reckoned by means of the ephemeris based on the photometric times of primary eclipse (Eq. (1)). The sinusoidal solution (solid and dashed lines in Fig. 2 for the less massive and the more massive component, respectively) has been determined for a circular orbit and fits very well all the observations.

The orbital parameters of the system, derived from the radial velocity solution and from the solution of the light curve (Lanza et al. 2002), are listed in Table 3, where P and S indices refer to the *primary* (more massive) and the *secondary* (less massive) component of the system, respectively.

The first solution of the radial velocity curve was given by Joy (1931). He found a value for the semi-amplitude

Table 2. Radial velocity measurements of RT Lac.

HJD (2 450 000+)	Phase	V_P (km s^{-1})	Error	V_S (km s^{-1})	Error
1743.5991	0.0400	−39.71	6.57	−84.48	4.98
1743.6281	0.0457	−31.80	8.66	−88.21	4.85
1744.5774	0.2328	−13.40	4.96	−170.00	3.57
1767.5380	0.7585	−102.87	8.45	60.65	3.86
1768.5282	0.9537	−71.13	7.81	−11.72	4.31
1768.5861	0.9651	−75.66	4.09	−20.79	2.90
1769.5764	0.1603	−24.10	5.35	−154.25	3.91
1771.5245	0.5443	—	—	−35.39	4.21
1772.5861	0.7535	−104.27	8.21	58.52	4.16
1775.5295	0.3337	−12.21	4.84	−155.40	3.98
1776.5106	0.5271	—	—	−41.49	1.86
1777.5255	0.7271	−100.88	7.91	59.18	3.28
1806.4630	0.4309	−37.45	7.03	−111.67	3.40
1807.4441	0.6243	−84.52	6.85	18.08	3.19
1808.4525	0.8230	−101.49	6.80	45.85	3.58
1809.4354	0.0168	−46.72	3.55	−72.56	2.71
1810.4975	0.2261	−12.35	5.41	−176.17	4.34
1812.5246	0.6257	−87.92	8.67	15.19	3.38

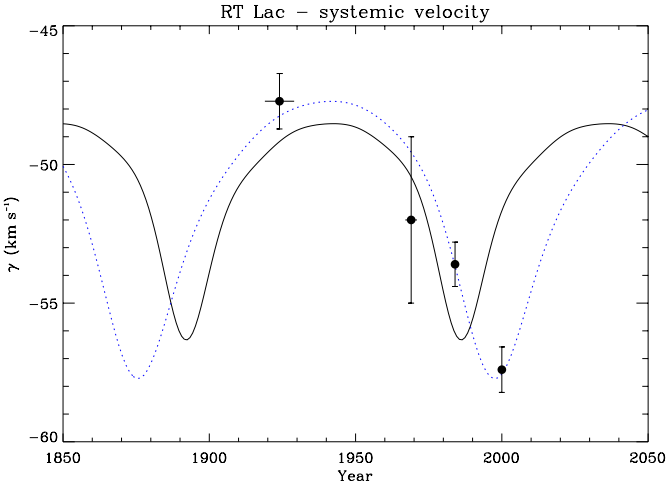

Fig. 3. The systemic RV of RT Lacertae in four observing seasons is displayed by filled dots. The orbital solution derived by İbanoğlu et al. (2001) is shown with a continuous line. The dotted line represents a solution with a larger period and mass of the third body, which fits better the observations.

Table 3. New orbital and physical parameters of RT Lac.

Element	
γ (km s^{-1})	-57.43 ± 0.82
K_S (km s^{-1})	115.04 ± 1.28
K_P (km s^{-1})	46.59 ± 2.17
M_S/M_P	0.405 ± 0.118
$a_S \sin i$ (km)	$8.03 \times 10^6 \pm 0.89 \times 10^5$
$a_P \sin i$ (km)	$3.25 \times 10^6 \pm 1.51 \times 10^5$
$M_S \sin^3 i$ ($M_\odot$)	0.64 ± 0.05
$M_P \sin^3 i$ ($M_\odot$)	1.58 ± 0.06
i	$89\overset{\circ}{.}0$[a]
R_S ($R_\odot$)	4.81 ± 0.14[b]
R_P ($R_\odot$)	4.41 ± 0.13[b]

[a] From Lanza et al. (2002).
[b] Fractional radii from Lanza et al. (2002).

of the hotter component $K_{hot} = 62.5 \pm 1.9$ km s^{-1}, much higher than all the subsequent radial velocity curves. For the less massive star, whose lines are much better seen in his spectra, he found a value $K_{cool} = 116.0 \pm 1.4$ km s^{-1} which is instead in very good agreement with subsequent determinations. Huenemoerder & Barden (1986) give $K_{hot} = 53.0 \pm 1.6$ km s^{-1} and $K_{cool} = 113.5 \pm 1.6$ km s^{-1}.

Popper (1991) published radial velocity measurements mainly based on Lick blue-violet and visual spectrograms obtained from 1967 to 1971. Notwithstanding the scatter of his data, the semi-amplitudes K_{hot} and K_{cool} he measured from absorption lines in the blue-violet and optical region and from the Ca II emission lines, are in very good agreement between themselves and very close to the values determined by us. The final solution adopted by Popper is $K_{hot} = 46 \pm 2$ km s^{-1}, $K_{cool} = 115 \pm 3$ km s^{-1}, and $\gamma = -52 \pm 3$ km s^{-1}.

As far as the systemic radial velocity γ is concerned, it is worth noticing that, starting from the early observations of Joy (1931), γ shows a steady decrease from -47 km s^{-1} to -57 km s^{-1} over about 80 years. Although Joy's measurements are affected by significant errors, due to the technique of measuring radial velocities from the position of a few individual lines in a very crowded spectral region, and due to the low resolution, he evaluated for γ a probable error of ± 1.6 km s^{-1}. Moreover, the subsequent determination made by Wilson (1941) of $\gamma = -47.72 \pm 0.64$ km s^{-1} with Joy's data, does support such a value of γ around 1920. The intermediate values of γ found by Popper (1991) in 1967–1971 ($\gamma = -52$ km s^{-1}) and by Huenemoerder & Barden (1986) in 1984 ($\gamma = -53.6 \pm 0.8$ km s^{-1}) do indicate that a real variation of the systemic velocity, much larger than 3σ, has indeed occurred.

From the O–C diagram for times of minimum light presented by Keskin et al. (1994) and by İbanoğlu et al. (2001) a cyclic variation with a period of the order of one century, over which minor variations are superimposed, is apparent. Keskin et al. (1994) attributed this variation to a light-time effect due to the presence of a third body which turns around the inner binary with a period of ∼81 yr. İbanoğlu et al. (2001) have re-analyzed Keskin et al. and their own O–C data inferring for this hypothetical third body an orbital period of about 94 yr, a separation from the inner binary of 11.3 AU and a mass ranging from 1.2 to 1.5 solar masses (for an inclination going from 90° to 60°).

In this hypothesis we expect a variation of the systemic velocity with a semi-amplitude $k_{12} = 3.5$–3.9 km s^{-1}, depending on the inclination assumed. This value is too small to reproduce the observed velocity variation, as

shown in Fig. 3, where the systemic velocity measured in the four different epochs with superimposed the orbital solution proposed by İbanoğlu et al. (2001) is shown. A solution with a slightly lower eccentricity ($e = 0.35$) and the same ω, but with a longer period (122 yrs), a different initial epoch and a larger mass for the third body ($M_3 = 2\,M_\odot$ which yields a larger velocity semi-amplitude) fits much better to the observations. However, if belonging to a normal star, the spectral lines of such a large mass third body should be very easily detected in our spectra of RT Lac. The same should have occurred for a star with the mass derived by İbanoğlu et al. (2001). However, at the distance of RT Lac, the semi-major axis of the orbit of the mass-center of the inner binary should be about 0.″05 which could be observable with a long series of accurate astrometric positions.

3.2. Hα emission profiles

The Hα line is an important indicator of chromospheric activity. Only the very active binaries show Hα emission always above the continuum (e.g. II Peg, V711 Tau, UX Ari, XX Tri, AR Psc); in less active stars only a filled-in absorption line is observed. For some objects the Hα line goes from filled-in absorption to emission during flare events (Catalano & Frasca 1994) or during activity variations over longer time scales, like those induced by rotational modulation or cycles.

The situation is more complex in a double-lined system in which both spectra are simultaneously seen and shifted at different wavelengths, according to the orbital phase. Therefore, in order to extract a valid information about the chromospheric contribution, a comparison with a "synthetic" spectrum constructed with two stellar spectra that mimic the two components of the system in absence of activity is needed.

In addition to the sensitivity to chromospheric layers, Hα emission is also a good diagnostic of inter-system matter in the form of gas streams, transient or classical accretion disks and rings in mass-transferring binaries like those of the Algol type, in which the cooler star fills-in its Roche lobe and transfers mass to the hot companion (see e.g. Richards & Albright 1999). Evidence for inter-system matter have been also recently reported by Marino et al. (2001) for HR 7428, a long-period detached atypical RS CVn binary composed of a bright K giant and an A-type star.

RT Lac is a particular case because it is classified as a RS CVn binary due to the late spectral type of both stars, but has a component that is very close to the Roche critical surface, so that some mass transfer through the Lagrangian L_1 point could occur if some mechanism is able to bring matter very close to this limit. It is then important to understand the physical meaning of the variable Hα emission displayed by RT Lac and to try to discriminate between chromospheric activity of the two components and possible inter-system matter contributions.

Hα absorption with possible filling-in of the line in RT Lac at phases between 0.ᵖ89 and 0.ᵖ92, was reported by Liu & Tan (1986). However, the first detailed study on the Hα behaviour of RT Lac was made by Huenemoerder (1985). Applying the spectral subtraction technique to moderate-resolution spectra, he found a very variable Hα line with excess emission stronger at phases around 0.ᵖ25 coming essentially from the fainter (more massive) component that he classified as K1, while the G9 (less massive) component displayed always a very low or null emission excess in his spectra. This phase-dependent behaviour was explained as due to a hot spot produced onto the trailing hemisphere of the more massive component, at about 40° from the axis joining the two components. This feature alone, however, is not able to explain the Hα emission observed also at other phases, and chromospheric activity is then invoked. An active chromosphere of the more massive star is also indicated by the excess emission observed by Huenemoerder (1985, 1988) in the cores of Ca II IRT lines at the velocity corresponding to this star.

He also found a strong extra-absorption ($EW \simeq 1$ Å) around phase 0.ᵖ5 (i.e. near the occultation of the more massive star) in one spectrum in November 1982 and in five spectra in September 1983. He suggested the presence, at those epochs, of "a body of cool hydrogen extending outwards, towards or through the external Lagrangian point L_2" so that the observed excess absorption should be associated with the less massive G9 star, being the more massive component nearly completely occulted at these phases.

In a subsequent paper, Huenemoerder & Barden (1986) analyzed contemporaneous optical and UV spectra of RT Lac and proposed a hot spot as responsible for the Hα emission variation. Its maximum visibility should have occurred at phase 0.ᵖ4, but, at about this phase, the extra-absorption effect begins to be visible. The authors in that occasion attributed the extra-absorption feature to a turbulent region around the stream-impact area. The strongest Hα emission is seen instead between phase 0.ᵖ6 and 0.ᵖ8, again coming from the more massive component. However, they observed Mg II emission from both components and pointed out the difficulty of giving a clear picture of the system. They also argued about the possibility that chromospheric emission could be responsible for the steady Hα variation with phase (and between the average levels of the two components), because of the "mixed" (collisional/photoionization) control of the line at the temperature regimes of the G-K stars. The models of Cram & Mullan (1985) show that the presence of a chromosphere increases the strength of the Hα absorption in late-type stars, unless the pressure is high enough to induce a collisional control of the line which goes into emission. Then the Hα variations could be due to the presence of large inhomogeneities in the chromosphere of the components of RT Lac with a large intensity contrast in Hα with respect to the quiet chromosphere.

Frasca & Catalano (1994) report on a faint Hα emission observed in two low-resolution (≃1 Å) spectra of

RT Lac acquired in 1989. The spectrum at phase $0^{\rm p}.86$, that is displayed in their paper, clearly shows Hα emission above the continuum from the more massive component and a filled-in Hα line from the less massive one.

Two Hα spectra acquired at phases $0^{\rm p}.33$ and $0^{\rm p}.68$ by Fernández-Figueroa et al. (1994) clearly show an emission feature above the continuum that, according to the observed Doppler shifts, is related to the more massive component, while an absorption more or less filled-in by emission can be associated with the less massive star. Difference Hα emission EW for these spectra are given by Montes et al. (1995) with values of 0.14–0.42 Å for the less massive component (listed as hotter star in their paper) and 0.37–0.39 Å for the more massive one. However, the weights they used (0.47/0.53) are somewhat different from those used by us and Huenemoerder & Barden (1986).

Both components display Ca II H & K emission cores (Popper 1942, 1991), and the less massive component usually shows weaker emission. Four spectra of RT Lac in the Ca II H & K region (Armentia et al. 1990) show emission core from both stars and, in one case ($\phi = 0.87$), with comparable intensities. Phase variation of total Ca II emission was also reported by Droppo & Milone (1976).

Our observations of RT Lac are well distributed in orbital phase and were obtained at a spectral resolution (0.45 Å) comparable to that of Huenemoerder & Barden (1986). In addition to RT Lac, some inactive stars of spectral type similar to that of each component of the system have been observed with the aim of producing a series of inactive synthetic spectra at the various phases of RT Lac observations. We have used μ Her (G5 IV) to reproduce the hotter component, and ϵ Cyg (K0 III) for the cooler one. These standard stars were selected on the basis of the spectral classification revised by Popper (1991) and of the agreement of their $B-V$ colors with those of the two component of RT Lac (İbanoğlu et al. 2001). For the construction of the inactive templates, the spectra of μ Her and ϵ Cyg have been rotationally broadened by convolution with the appropriate rotational profile and then have been co-added, properly weighted and Doppler-shifted according to the RV solution derived in the previous subsection.

The contributions of the two stars to the combined spectrum at the Hα wavelength have been evaluated from the relative areas of the Gaussians fitting the cross-correlation peaks of the RT Lac components (see Fig. 1). Average contributions of 0.65 and 0.35, for the less massive and the more massive star respectively, have been obtained. These weights are in very good agreement with those derived by Huenemoerder (1985) and Huenemoerder & Barden (1986).

The projected rotational velocities $v \sin i$ can be deduced from the light curve solution (fractional radii, orbital/rotational period, and inclination) and our RV solution, which gives the absolute radii through the system separation. We find 44 $\mathrm{km\,s^{-1}}$ and 48 $\mathrm{km\,s^{-1}}$ for the more massive and the less massive component, respectively. We have checked the consistency of the $v \sin i$ that can be measured on our spectra with the calculated $v \sin i$. We have converted the $FWHM$ of the Gaussians fitted to the CCF peaks into $v \sin i$'s by means of a calibration $FWHM - v \sin i$ established through CCFs of the RV standard star 31 Aql with other spectral-type standard stars artificially broadened. From our spectra, taking into account only those in which the lines of the two components are well separated, we found 36 ± 7 $\mathrm{km\,s^{-1}}$ for the primary and 48 ± 4 $\mathrm{km\,s^{-1}}$ for the secondary star. The latter value is in very good agreement with the calculated one, while for the primary star we have a slight discrepancy. It is interesting to notice that the projected rotational velocities derived by Huenemoerder (1985), $v \sin i = 38/47$ $\mathrm{km\,s^{-1}}$, and by Huenemoerder & Barden (1986), $v \sin i = 34 \pm 7/42 \pm 3$ $\mathrm{km\,s^{-1}}$, are fully consistent, within the errors, between themselves and with our values. The values of $v \sin i$ measured by us have been adopted for the construction of the inactive templates.

During the eclipses the weights have been properly corrected taking into account the light contribution of each star at each phase. In addition, the slight distortion and shift of line profiles produced during the eclipses by the occultation of a portion of the stellar disk of one component by the companion has been also taken into account following the method proposed by Frasca et al. (2000).

To define the net Hα emission of the two components we have subtracted the synthetic spectrum from each RT Lac spectrum. In the difference spectrum the absorption lines cancel out and the excess emission of both components in the Hα core appears as a positive residual well above the noise (Figs. 4–6). In these figures, a sample of Hα profiles at different phases is shown. In the left-side panels the observed spectra are displayed by thick lines, while the synthetic ones are reproduced by the thin lines. In the right-side panels the differences are shown. The phases of observations and the wavelength of the Hα centers of the more massive (P) and less massive (S) component are also marked.

From the observed spectra a strong Hα emission corresponding to the primary (more massive) component, which is always above the local continuum with the exception of spectra taken near to the eclipses, is apparent. The secondary (less massive) component displays instead a Hα line only partially filled-in by a variable emission which becomes practically negligible at phase $\simeq 0^{\rm p}.75$ (Fig. 5). The difference Hα emission peaks from both components are centered at wavelengths corresponding to the star photospheric centers. The shape and width of these residual emission profiles are consistent with the residual Hα profiles observed in several other detached RS CVn binaries for which a pure chromospheric origin of the Hα line has been inferred (Frasca et al. 1998; Catalano et al. 2000; Frasca et al. 2000).

However, in the residual spectra acquired on August 11th at phases about $0^{\rm p}.954$ and $0^{\rm p}.965$, i.e. at the beginning of the eclipse of the less massive component, a blue-shifted extra absorption is visible. This feature is no longer visible either at the eclipse center (September 21th) nor at the

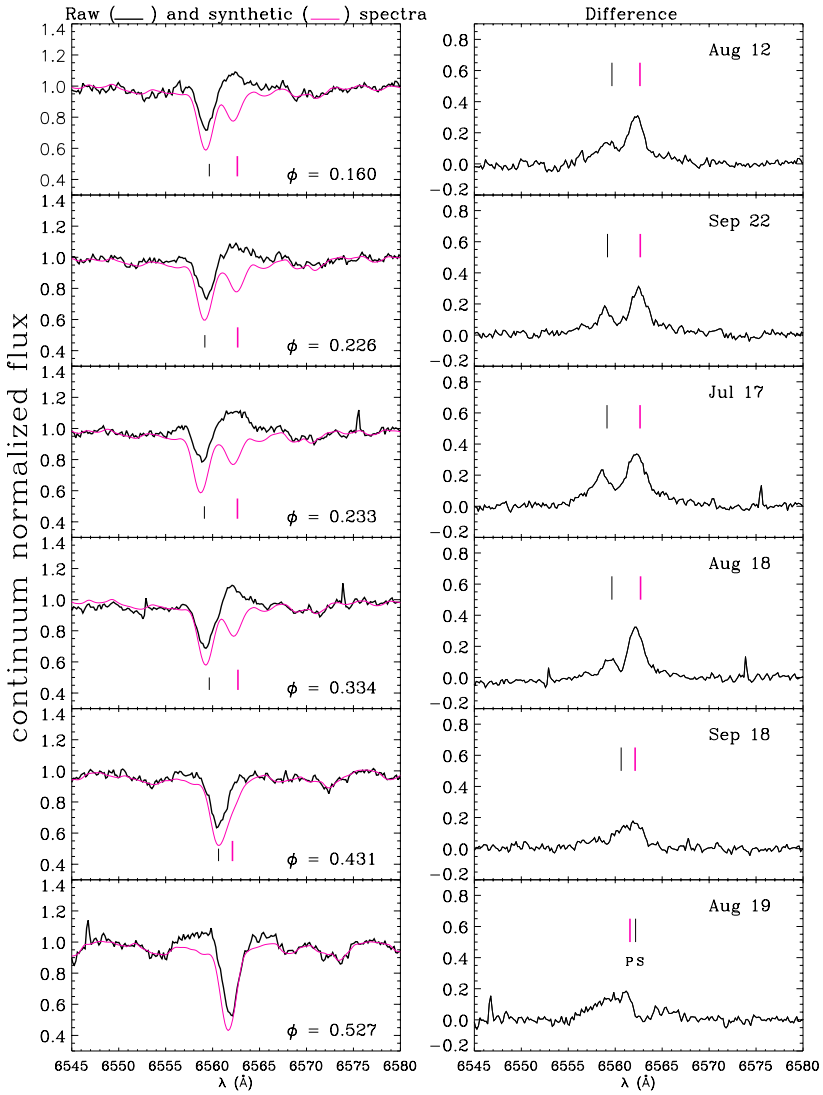

Fig. 4. Sample of Hα spectra of RT Lac. In the left panels the observed spectra are displayed by a thick line, while the synthetic ones are reproduced by thin lines. In the right-side panels the differences are shown. The phases of observations and the wavelength of the Hα centers of the more massive (P) and less massive (S) component are also marked.

egress (July 16th, $\phi = 0\overset{p}{.}040-0\overset{p}{.}046$) when only a filled-in Hα profile, just reaching the continuum, is present. This observation indicates that some extended matter around the smaller component or within the binary system should be present and that it is projected against the G9 star at 0.95 phase with a velocity approaching to the observer. A similar feature was observed in AR Lac (Frasca et al. 2000) at about the same phase, but the extra-absorption was seen red-shifted. In that case, the extra-absorption was interpreted as produced by a prominence-like structure. In the present case of RT Lac, the hypothesis of a steady or transient disk around the smaller component and corotating with it, as observed in several Algol-type binaries (Richards & Albright 1999), can be ruled out as the cause for the observed extra absorption. In fact, at phases around the first contact ($0\overset{p}{.}95$), one has the receding side of the accretion disk projected against the occulted star so that a red-shifted, not a blue-shifted absorption should be observed. This feature could then be due to another region of inter-system matter, like, for example, a stream flowing from the less massive to the companion through L_1, which is seen projected against the stellar disk of the former star at this phase, and with a blue-ward velocity. However, the hypothesis of an extended structure, like a prominence linked to the primary star, cannot be excluded.

The most striking feature, however, is the disappearance of emission just during the eclipse of the smaller component ($\phi = 0\overset{p}{.}5$) which demonstrates that the bulk of emission is coming presumably from its chromosphere or from a region very close to the surface of this star. At the eclipse center, only a very faint and broad emission remains. The spectrum of Aug. 19 is very similar to that observed by Huenemoerder & Barden (1986) at phase $0\overset{p}{.}457$ and it is reminiscent of spectra of some Algol stars at analogous phases, namely CX Dra, TX UMa, U CrB (Richards & Albright 1999) in which the double-peaked broad emission observed is attributed to transient disks

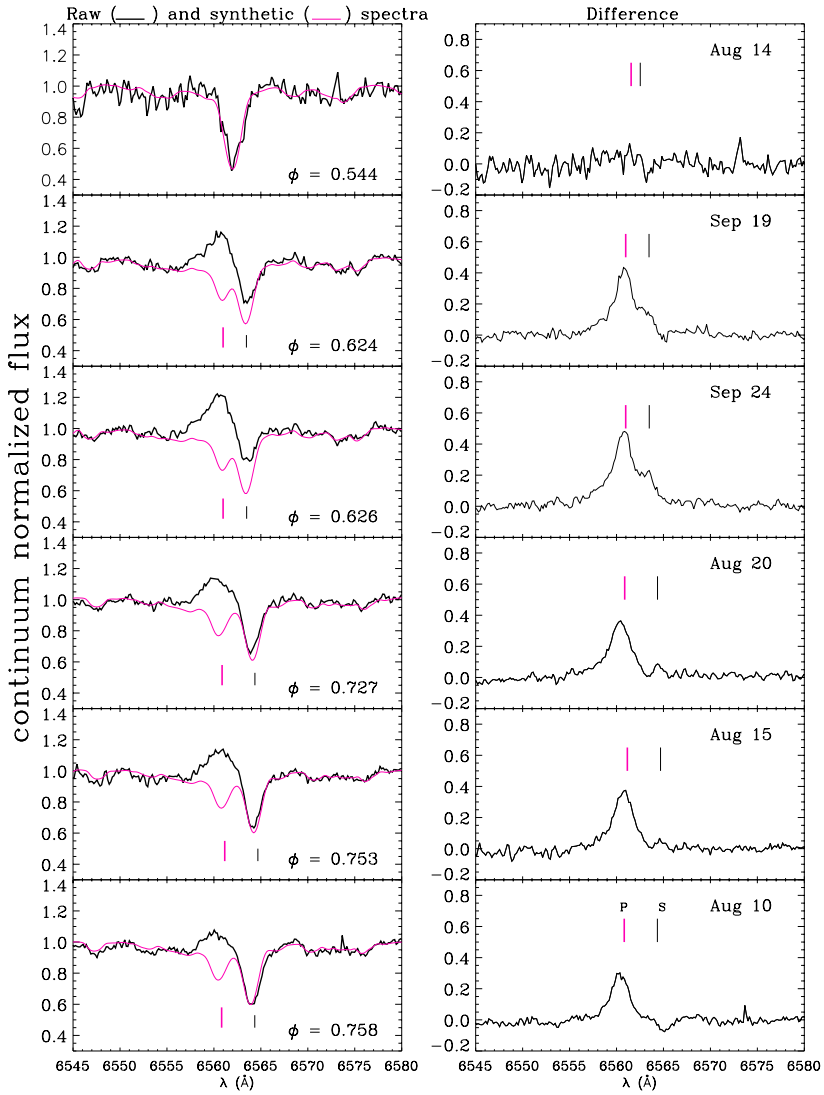

Fig. 5. Sample of Hα spectra of RT Lac. In the left panels the observed spectra are displayed by a thick line, while the synthetic ones are reproduced by thin lines. In the right-side panels the differences are shown. The phases of observations and the wavelength of the Hα centers of the more massive (P) and less massive (S) component are also marked.

around the hot components. For RT Lac, however, the effect is much less evident than in these Algol systems, as one can expect from a less efficient mass transfer of the G9 star, which is not completely filling its Roche lobe. Also the much lower excitation/ionization rate of the circumstellar material from the G5 component of RT Lac, that is much cooler than typical hot components of Algol systems, would make the disk emission less prominent.

3.3. Hα EW and photometric behaviour

The net equivalent width (EW) of the "total" Hα emission has been evaluated on the difference spectra integrated along the entire residual emission profile. This cumulative integration has the drawback that it merges the emission contribution of both stars, but it can be done at each phase, even if the two Hα residual profiles are too blended to be separated. The errors on the measured EW were estimated determining the S/N in two windows on the right- and left-hand side of Hα in the difference spectrum and multiplying it for the width of the integration range.

Equivalent widths (EW) calculated from emission excess, together with their corresponding heliocentric JD, phase, and weights (W_C), are listed in Table 4 and are displayed, as a function of orbital phase, in Fig. 7 together with the contemporaneous V-band light curve (dots) and the light curve solution (Lanza et al. 2002).

These EWs are relative to the local continuum that is a mixture of the primary and secondary star spectra whose weights vary during the eclipses, affecting the measured equivalent widths that, in any case, contain a "cumulative" information about the two stars.

In Fig. 7 the decrease of EW in coincidence with both eclipses is apparent. For spectra just before the eclipse of the less massive component (at phase $\simeq 0\overset{p}{.}95-0\overset{p}{.}96$), the extra absorption is mainly responsible for the decrease of the cumulative EW. For spectra close to phase $0\overset{p}{.}5$

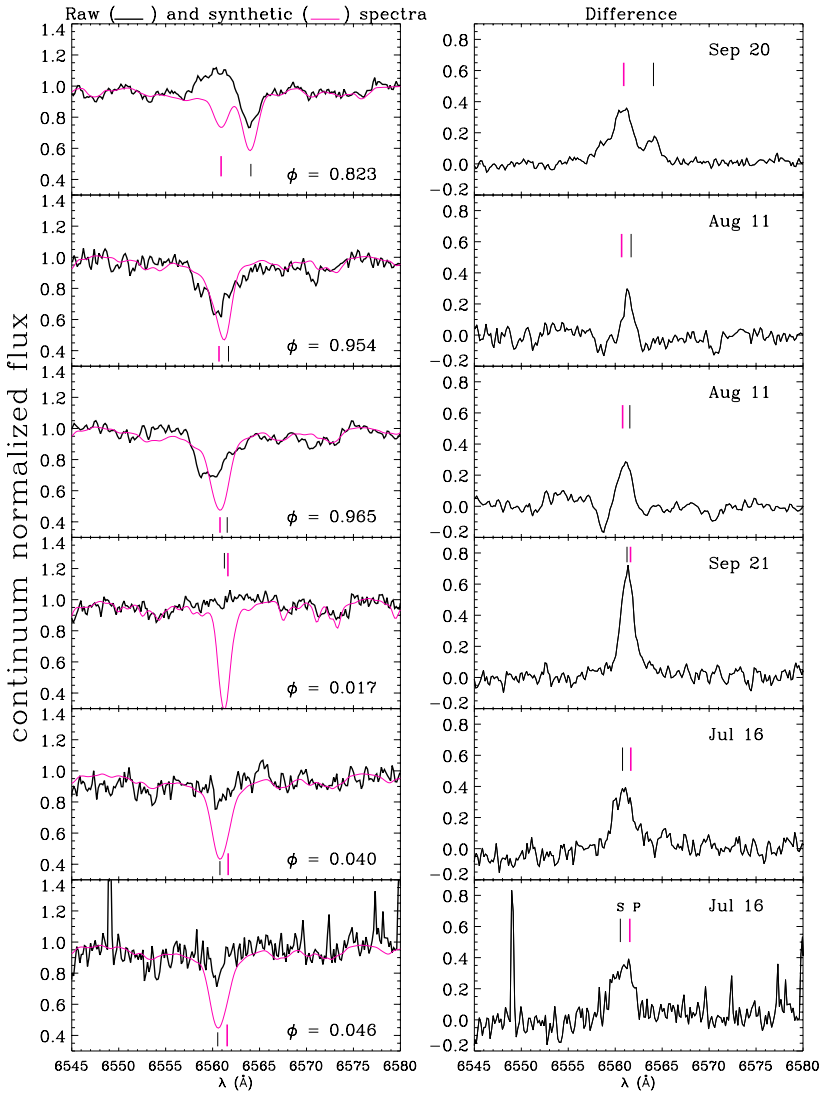

Fig. 6. Sample of Hα spectra of RT Lac. In the left panels the observed spectra are displayed by a thick line, while the synthetic ones are reproduced by thin lines. In the right-side panels the differences are shown. The phases of observations and the wavelength of the Hα centers of the more massive (P) and less massive (S) component are also marked.

the eclipse of the chromosphere of the more active star presumably plays the more important role in the EW decrease.

In order to disentangle the Hα variation of the two stars, we have performed a "deblending" of the two residual emission profiles in configurations of great or moderate wavelength separation by fitting two Lorentian or Voigt functions. An example of the application of this procedure is shown in Fig. 8.

The equivalent widths derived in such a way have been corrected dividing them by the weight of the corresponding component so to have the net Hα EW of each star with respect to its local continuum as if it were a single star. Resulting EWs are listed in Table 4 as $EW_{\rm P}$ and $EW_{\rm S}$ for the primary (more massive) and secondary component, respectively. These values are also displayed versus orbital phase in Figs. 9, 10, together with the relative spot area deduced from the spot model of the corresponding light curve (Lanza et al. 2002) with Tikhonov regularization algorithm.

The first relevant result of the simultaneous photometric and Hα monitoring is that the star that is more active in Hα at this epoch, namely the primary component, turns out to be also the more heavily spotted. This reinforces the hypothesis of a prevalent chromospheric origin for the observed Hα emission.

Furthermore, as can be easily seen in Fig. 9, the hemisphere of the primary star facing the observer at phase around $0\overset{\rm p}{.}75$ is the brightest in Hα and results to be that with the greatest spot concentration. This means that the Hα emission variation in this star can be attributed to bright chromospheric plages that are spatially associated with the photospheric spots.

For the secondary star a smooth phase-dependent variation of Hα emission is seen (Fig. 10), but the photometric solution gives two active regions at different longitudes, the smaller of which, at about phase $0\overset{\rm p}{.}0$, is fairly

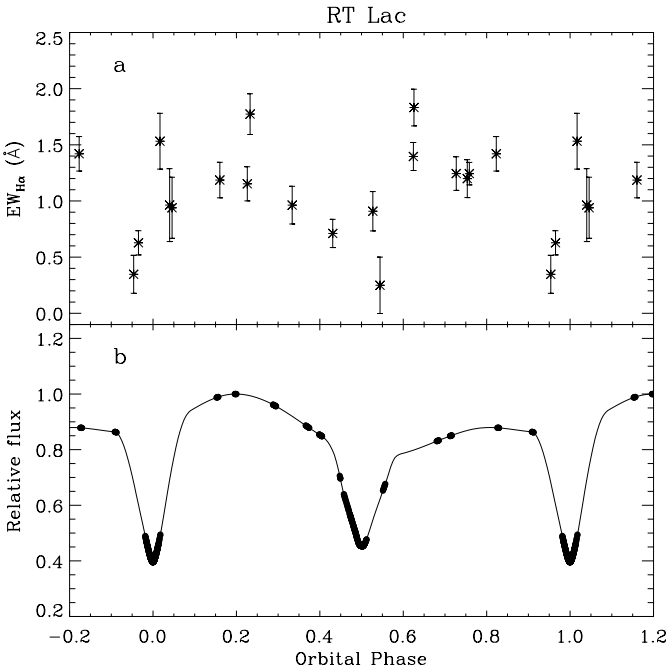

Fig. 7. Hα EW **a)** and V light **b)** curve of RT Lac in 2000. The light-curve solution performed by Lanza et al. (2002) is also displayed in the lower panel by continuous line.

Table 4. Hα equivalent widths measurements of RT Lac obtained in 2000.

HJD 2 450 000+	Phase	w_C	EW_T (Å)	Error (Å)	EW_P (Å)	EW_S (Å)
1743.5991	0.0400	0.367	0.963	0.325	—	—
1743.6281	0.0457	0.413	0.939	0.272	—	—
1744.5774	0.2328	0.650	1.774	0.181	3.751	0.925
1767.5380	0.7585	0.650	1.244	0.101	3.931	0.042
1768.5282	0.9537	0.418	0.347	0.169	—	—
1768.5861	0.9651	0.325	0.628	0.108	—	—
1769.5764	0.1603	0.650	1.186	0.158	2.717	0.566
1771.5245	0.5443	0.811	0.249	0.251	—	—
1772.5861	0.7535	0.650	1.199	0.169	3.963	0.048
1775.5295	0.3337	0.650	0.963	0.168	2.509	0.209
1776.5106	0.5271	0.900	0.909	0.175	—	—
1777.5255	0.7271	0.650	1.244	0.150	4.160	0.085
1806.4630	0.4309	0.703	0.711	0.126	—	—
1807.4441	0.6243	0.650	1.396	0.125	4.394	0.151
1808.4525	0.8230	0.650	1.420	0.154	4.154	0.362
1809.4354	0.0168	0.170	1.532	0.248	—	—
1810.4975	0.2261	0.650	1.153	0.152	2.826	0.508
1812.5246	0.6257	0.650	1.832	0.163	5.614	0.332

coincident with the maximum Hα emission. This photospheric active region was also observed in 1999 (see Lanza et al. 2002), when a much denser coverage of the light curve was obtained, and this spot turned out to be the bigger one. The analysis of photometric data taken in 2000 could have suffered from relatively poor phase coverage, in particular at the ingress and egress of primary eclipse ($\phi = 0\overset{p}{.}0$), so that the photospheric spot seen at this phase could be still the more prominent.

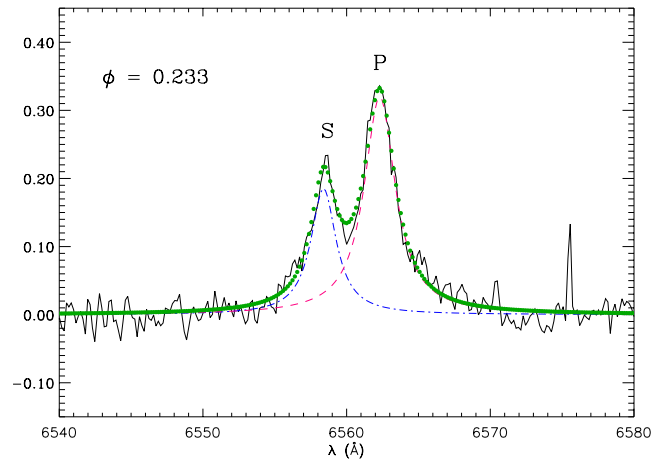

Fig. 8. An example of "deblending" of a double-peaked Hα residual emission. The fit to the difference spectrum (continuous line) made up by two Lorentian function is shown by dots. The deconvolved emission profiles of the primary (more massive) and secondary component are displayed by dashed and dot-dashed line, respectively.

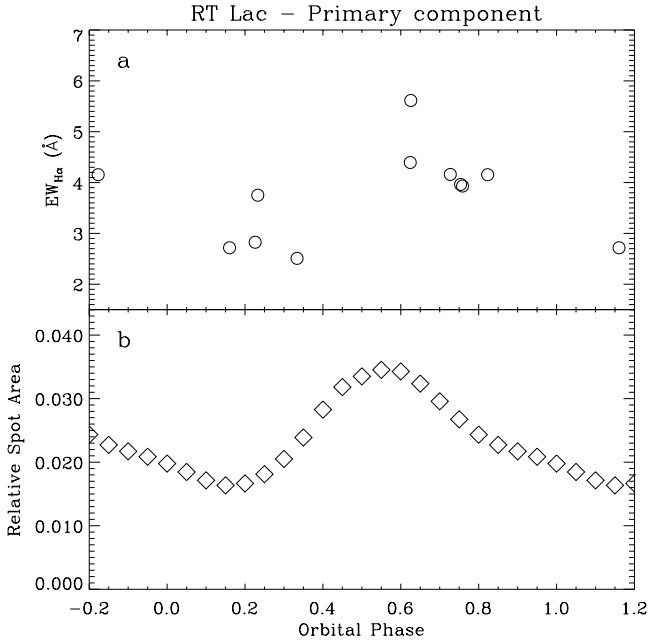

Fig. 9. Hα EW_P for the primary more massive component of RT Lac system **a)** and relative spot area **b)** versus phase.

So, it seems that a spatial association between photospheric and chromospheric active regions exists for the secondary star, too.

4. Conclusions

A large set of medium-resolution spectra has allowed us to measure with good accuracy the radial velocity of both components of RT Lac. A new solution of the radial velocity curve has been given and orbital parameters of the system have been derived. The values we find are all in good agreement with previous determinations, with the exception of the barycentric radial velocity γ which

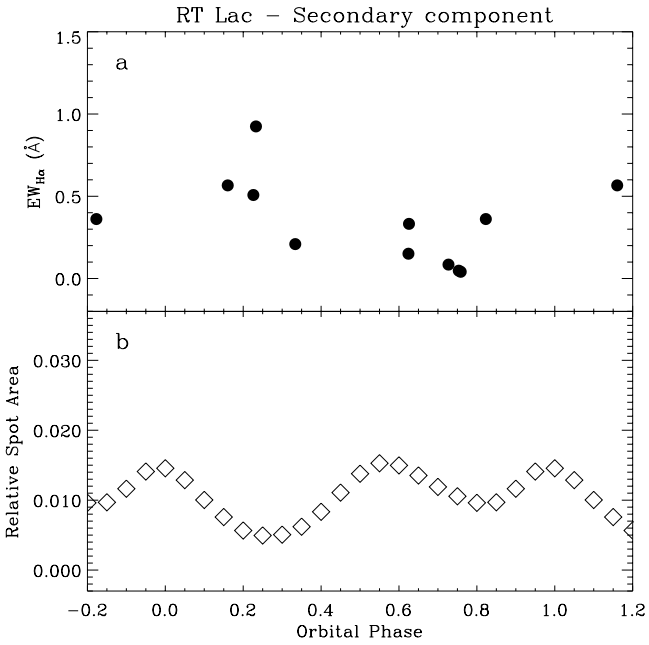

Fig. 10. Hα EW_S for the secondary less massive component of RT Lac system **a)** and relative spot area **b)** versus phase.

displays a clear decreasing trend from the first RV curve obtained by Joy (1931), around 1920, up to now. This behaviour is compatible with the hypothesis of a third body orbiting around the barycenter of the inner binary with a period of the order of 100 years. However, no clue of the presence of a third star from spectroscopic or photometric observations has been given until now.

A careful analysis of the Hα profiles, making use of the "spectral synthesis" method, has shown Hα emission from both components, the more massive one having a Hα flux about ten times greater than the companion. The shape and width of these residual emission profiles are consistent with the residual Hα profiles observed in several other detached RS CVn binaries for which a pure chromospheric origin of the Hα line has been inferred (Frasca et al. 1998; Catalano et al. 2000; Frasca et al. 2000). Extended Hα-absorbing matter has been detected just before the eclipse of the less massive component, but it remains unclear if such a region is related to mass transfer within the system through L_1 or is simply produced by the strong activity of the more massive component, i.e. a prominence-like structure.

Rotational modulation of the Hα emission from both components has been also detected. Thanks to the contemporaneous photometry and to an accurate spot modelling, we can state that the star that displays higher Hα activity, i.e. the primary more massive component, is also more heavily spotted at the epoch of our observations.

In addition, a good spatial association between photospheric and chromospheric active regions has been established, at least for the more active primary star.

Acknowledgements. This work has been supported by the Italian *Ministero dell' Università e della Ricerca Scientifica e Tecnologica* and by the *Regione Sicilia* which are gratefully acknowledged. Ö. Çakırlı gratefully acknowledges the Scientific and Technical Resource Council of Turkey, whose financial support has allowed his stay in Catania and the gathering of the spectroscopic data. We would like to thank the referee for his/her useful comments.

References

Armentia, J. E., Fernández-Figueroa, M. J., Cornide, M., de Castro, E., & Fabregat, J. 1990, in Proc. NATO Adv. Study Inst., Active Close Binaries, ed. C. İbanoğlu (Kluwer Academic Publ.), 551
Catalano, S., & Frasca, A. 1994, A&A, 287, 575
Catalano, S., Rodonò, M., Cutispoto, G., et al. 2000, in NATO Sci. Ser. C: Math. and Phys. Sci. 544, Variable Stars as Essential Astrophysical Tools, ed. C. İbanoğlu (Kluwer Academic Publishers), 687
Cram, L. E., & Mullan, D. J. 1985, ApJ, 294, 626
Droppo, J. L., & Milone, E. F. 1976, IBVS, 1130
Eaton, J. A., & Hall, D. S. 1979, ApJ, 227, 907
Evans, D. S. 1967, in Determinations of radial velocities and their applications, ed. A. H. Batten, & J. F. Heard (Academic Press, London), Proc. IAU Symp., 30, 57
Evren, S. 1989, Ap&SS, 161, 303
Fernández Figueroa, M. J., Montes, D., De Castro, E., & Cornide, M. 1994, ApJS, 90, 433
Frasca, A., & Catalano, S. 1994, A&A, 284, 883
Frasca, A., Catalano, S., & Marilli, E. 1998, in The 10th Cambridge Workshop on Cool Stars Stellar Systems and the Sun, ed. R. A. Donahue, & J. A. Bookbinder (Sheridan Books, Chelsea, Michigan), ASP Conf. Ser., 154, 1421
Frasca, A., Marino, G., Catalano, S., & Marilli, E. 2000, A&A 358, 1007
Hall, D. S. 1976, in Multiple Periodic Variable Stars, ed. W. S. Fitch (Reidel Publ.), Proc. IAU Coll., 29, 287
Huenemoerder, D. P. 1985, AJ, 90, 499
Huenemoerder, D. P. 1988, PASP, 100, 600
Huenemoerder, D. P., & Barden, S. C. 1986, AJ, 91, 583
İbanoğlu, C., Evren, S., Taş, G., Devlen, A., & Çakırlı, Ö. 2001, A&A, 371, 626
Joy, A. H. 1931, ApJ, 74, 101
Keskin, V., İbanoğlu, C., Akan, M. C., Evren, S., & Tunca, Z. 1994, A&A, 287, 817
Lanza, A. F., Catalano, S., Rodonò, M., et al. 2002, A&A, in press
Liu, X.-F., & Tan, H.-S. 1986, Acta Astron. Sin., 6, 132
Marino, G., Catalano, S., Frasca, A., & Marilli, E. 2001, A&A, 375, 100
Milone, E. F. 1976, ApJS, 31, 93
Milone, E. F. 1977, AJ, 82, 998
Milone, E. F., & Naftilan, S. A. 1980, in Close binary stars: Observations and interpretation, Proc. of the Symp., ed. M. J. Plavec, & R. K. Ulrich (Dordrecht, D. Reidel Publishing Co.), 419
Montes, D., Fernandez-Figueroa, M.J., De Castro, E., & Cornide, M. 1995, A&A, 294, 165
Popper, D. M. 1942, PASP, 10, 292
Popper, D. M. 1976, IBVS, 1083
Popper, D. M. 1991, AJ, 101, 220
Richards, M. T., & Albright, G. E. 1999, ApJS, 123, 537
Tonry, J., & Davis, M. 1979, AJ, 84, 1511
Topping, J. 1972, Errors of Observation and Their Treatment (Chapman and Hall Ltd.), 89
Wilson, O. C. 1941, ApJ, 93, 29